Prepared for submission to JHEP

An improved moment QCD sum rule

Jin-Peng Zhang,[a] **Xu-Liang Chen,**[a] **Wei Chen**[a,b]

[a] *School of Physics, Sun Yat-Sen University, Guangzhou 510275, China*

[b] *Southern Center for Nuclear-Science Theory (SCNT), Institute of Modern Physics, Chinese Academy of Sciences, Huizhou 516000, China*

E-mail: chenwei29@mail.sysu.edu.cn

arXiv:2607.11536v1 [hep-ph] 13 Jul 2026

Abstract: QCD sum rules are among the most important non-perturbative tools in hadron physics, with the Laplace sum rule (LSR) and moment sum rule (MSR) being the two most commonly used formulations. Despite their widespread application, both approaches have significant shortcomings: the LSR relies on subjective criteria – namely OPE convergence and pole dominance – to constrain the parameter space, while the conventional MSR cannot extract the coupling constant of the interpolating current. More critically, the ground-state masses obtained from these two methods are often inconsistent. In this work, we propose an improved moment sum rule (IMSR) framework that resolves these issues simultaneously. Our method explicitly incorporates quark-hadron duality, which introduces the approximation condition on the OPE side and provides a natural a posteriori constraint on the parameters. We impose rigorous dependence conditions on the unphysical parameters (Q_0^2, n) to quantify and control their influence. As a result, our framework uniquely determines both the optimal value of the duality parameter and the ground-state mass, without invoking any ad hoc or subjective criteria. It also allows for the simultaneous extraction of the current coupling. Applying the IMSR to a pseudoscalar $ud\bar{d}\bar{s}$ tetraquark system, the results are in excellent agreement with our previous LSR analyses, validating the effectiveness of the proposed scheme. The IMSR method substantially enhances the robustness and reliability of QCD sum rules, effectively eliminating the subjectivity that has long plagued conventional formulations.

Contents

1 Introduction **1**

2 Laplace and moment QCD sum rules **2**
- 2.1 Laplace QCD sum rules 3
- 2.2 The conventional moment QCD sum rules 5

3 The improved moment QCD sum rules **6**
- 3.1 Motivation and core idea 6
- 3.2 Dependence conditions 9
- 3.3 General procedure 10

4 Numerical analysis and applications **11**

5 Discussion: Comparison with Laplace sum rules **14**

6 Summary **16**

A Proof and interpretation of $\eta(s_0, Q_0^2, n) > 1$ **17**

1 Introduction

QCD sum rules provide a well-established non-perturbative framework for studying hadron properties [1–3]. The central idea is straightforward: a correlation function is computed in the deep Euclidean region using the operator product expansion (OPE) and then linked to hadron phenomenology via the dispersion relation and quark-hadron duality. Over the years, this approach has been successfully applied to a wide range of hadrons, including conventional mesons and baryons, as well as exotic hadron states such as multiquarks, hybrids, and glueballs [4–13].

Several variants of the QCD sum rule method have been developed, each emphasizing different aspects of the framework. These include the Monte Carlo-based approach [14], the variable continuum threshold method [15], the inverse problem method [16, 17], the inverse matrix method [18–21], the resonance sum rules [22] and so on. Among these variants, the Laplace (or Borel) sum rule and the moment sum rule are the most widely used ones [1, 3, 23]. The Laplace method employs a Borel transform to suppress contributions from excited states and the continuum, whereas the moment method extracts the ground-state mass from moments of the correlation function. Although both approaches share the same theoretical starting point, they treat the phenomenological side differently, which often leads to numerically different results in practice.

The LSR relies on the existence of a "Borel window" where both OPE convergence and pole dominance are under control [24]. While this standard procedure often works well, the criteria for selecting the window are not unique. Being largely determined by human intervention, such criteria inevitably introduce procedural uncertainty and subjective bias into the final results. Furthermore, the pole contribution (PC) often varies significantly within the Borel window even when the extracted mass remains stable, raising questions about its physical meaning. The conventional MSR suffers from a different shortcoming. Although the hadron mass can be extracted, the coupling of the current to the ground state remains undetermined. Moreover, the obtained masses are systematically larger than those from LSR, suggesting that the method does not properly isolate the lowest-lying resonance.

In this work, we trace these issues to the treatment of quark-hadron duality. In the conventional moment approach, the OPE spectral density is integrated all the way to infinity, so the extracted mass inevitably receives contributions from higher states. By contrast, the LSR truncates the integral at a scale of the duality parameter s_0 via the quark-hadron duality assumption. This observation motivates us to propose an improved moment sum rule (IMSR) that explicitly incorporates quark-hadron duality. The improved framework retains the simplicity of the original moment method while restoring its connection to the ground state, thereby enabling the extraction of both the hadron mass and its coupling.

The core of the IMSR lies in the introduction of the approximation $\delta'_n(s_0, Q_0^2) \approx \delta'_{n+1}(s_0, Q_0^2)$ on the OPE side, which mirrors the phenomenological condition $\delta_n(s_h, Q_0^2) \approx \delta_{n+1}(s_h, Q_0^2)$. This approximation plays a twofold role: it aligns the OPE and phenomenological sides, and it inherently constrains the parameters (s_0, Q_0^2, n) as an a posteriori consistency check. A further key point is the identification of physical versus unphysical parameters. On this basis, we define dependence conditions and introduce a tolerance parameter to quantify the impact of the unphysical parameters. As a test of its validity, we apply the method to the fully light $ud\bar{d}\bar{s}$ tetraquark state. The results confirm its effectiveness.

The paper is organized as follows. In Section 2, we briefly review the LSR and conventional MSR, with emphasis on their limitations. Section 3 presents the framework of the improved moment sum rules, where we introduce the approximation $\delta'_n(s_0, Q_0^2) \approx \delta'_{n+1}(s_0, Q_0^2)$ and the dependence conditions. In Section 4, we perform a numerical analysis for the tetraquark state $ud\bar{d}\bar{s}$ to test the validity of our method. In Section 5, we perform a comparative analysis of the LSR and IMSR, emphasizing their similarities and distinctions. Finally, a summary and outlook are given in Section 6.

2 Laplace and moment QCD sum rules

In this section, we briefly review the two mainstream formulations of QCD sum rules that underpin our analysis: the LSR and the conventional MSR. For each approach, we outline the basic formalism, highlight its advantages, and discuss the inherent limitations that motivate the present study. Building on these discussions, we introduce the IMSR method in the following section.

2.1 Laplace QCD sum rules

We start from the two-point correlation function

$$\Pi(q^2) = \mathrm{i}\int \mathrm{d}^d x\ \mathrm{e}^{\mathrm{i}q\cdot x}\langle 0|T[J(x)J^\dagger(0)]|0\rangle, \tag{2.1}$$

where $J(x)$ is the interpolating current with the same quantum numbers as the physical state of interest. At the quark-gluon level, the correlation function can be computed in the deep Euclidean region ($Q^2 \equiv -q^2 \to \infty$) via the method of OPE

$$\Pi^{\mathrm{OPE}}(q^2) = \sum_i C_i(q^2,\mu)\langle O_i(\mu)\rangle, \tag{2.2}$$

where $\langle O_i(\mu)\rangle$ denote vacuum condensates, $C_i(q^2,\mu)$ are coefficient functions, and μ is the renormalization scale. The correlation function receives both perturbative and non-perturbative contributions, which encode the short- and long-distance QCD dynamics, respectively. The predictive power of the QCD sum rule approach can be systematically enhanced by incorporating higher-order perturbative and non-perturbative corrections.

On the phenomenological side, the correlation function in Eq. (2.1) can be described by the dispersion relation

$$\Pi^{\mathrm{PH}}(q^2) = \int_{s_N}^{\infty} \mathrm{d}s \frac{(q^2)^n \rho^{\mathrm{PH}}(s)}{s^n(s-q^2-\mathrm{i}0^+)} + \sum_{i=0}^{n-1} a_i (q^2)^i, \tag{2.3}$$

where s_N is the normal threshold and a_i are coefficients of subtraction terms. The hadronic spectral function can be parametrized by using the "narrow resonance" assumption

$$\rho^{\mathrm{PH}}(s) = \sum_X \delta(s-m_X^2)\langle 0|J|X\rangle\langle X|J^\dagger|0\rangle = f_X^2\delta(s-m_X^2) + \rho^h(s)\theta(s-s_h), \tag{2.4}$$

in which m_X and f_X are the hadron mass and coupling of the ground state respectively, and $\rho^h(s)$ represents contributions from the continuum and excited states with s_h denoting their threshold.

The cornerstone of the QCD sum rule approach is the assumption of quark-hadron duality, which posits that for s above the duality parameter s_0, the phenomenological spectral density $\rho^h(s)$ coincides with its OPE counterpart, $\rho^{\mathrm{OPE}}(s) = \frac{1}{\pi}\operatorname{Im}\Pi^{\mathrm{OPE}}(s)$. Local duality can be formulated as

$$\rho^h(s) = \frac{1}{\pi}\operatorname{Im}\Pi^{\mathrm{OPE}}(s)\theta(s-s_0), \tag{2.5}$$

while global duality takes the form

$$\int_{s_h}^{\infty} \mathrm{d}s \frac{\rho^h(s)}{s-q^2} = \int_{s_0}^{\infty} \mathrm{d}s \frac{\rho^{\mathrm{OPE}}(s)}{s-q^2}. \tag{2.6}$$

Obviously, the lack of knowledge about $\rho^h(s)$ [25] and "duality violating" [26, 27] inevitably introduce theoretical uncertainties.

Then the Borel transform

$$\hat{B} = \lim_{\substack{-q^2,n\to\infty \\ -q^2/n=M_B^2}} \frac{1}{\Gamma(n+1)}(-q^2)^{n+1}\left(\frac{\mathrm{d}}{\mathrm{d}q^2}\right)^n \tag{2.7}$$

is employed to both sides to suppress the contributions from higher excited states in Eq. (2.4), and eliminate the unknown subtraction terms in Eq. (2.3), and finally improve the convergence of OPE series. Subsequently, the Laplace QCD sum rules are obtained as

$$f_X^2\ \mathrm{e}^{-m_X^2/M_B^2} = \int_{s_N}^{s_0} \rho^{\mathrm{OPE}}(s)\ \mathrm{e}^{-s/M_B^2}\ \mathrm{d}s, \tag{2.8}$$

in which M_B^2 is the Borel parameter. Differentiating both sides of Eq. (2.8) with respect to $\frac{-1}{M_B^2}$, the hadron mass m_X of the lowest-lying resonance can be extracted to be

$$m_X(s_0, M_B^2) = \sqrt{\frac{L_1(s_0, M_B^2)}{L_0(s_0, M_B^2)}}, \tag{2.9}$$

where

$$L_k(s_0, M_B^2) = \int_{s_N}^{s_0} \rho^{\mathrm{OPE}}(s) s^k \mathrm{e}^{-s/M_B^2}\ \mathrm{d}s + \Pi^{\mathrm{NS}}(M_B^2), \tag{2.10}$$

and the last term $\Pi^{\mathrm{NS}}(M_B^2)$ denotes the high-dimensional OPE terms not associated with a spectral representation. With a fixed normal threshold s_N, the hadron mass in Eq. (2.9) depends only on the duality parameter s_0 and the Borel parameter M_B^2. These two parameters are conventionally constrained by imposing two criteria: the convergence of the OPE series in Eq. (2.2) and the dominance of the pole over the continuum in Eq. (2.4). Nevertheless, both criteria lack a unique and first-principle definition, and their implementation often involves subjective choices that differ from one analysis to another. Consequently, the value of s_0 and thus hadron mass m_X are not uniquely determined, introducing a certain degree of ambiguity and potential systematical bias into the final results.

On the other hand, the definition of pole contribution itself is questionable

$$\mathrm{PC}(s_0, M_B^2) := \frac{L_0(s_0, M_B^2)}{L_0(\infty, M_B^2)}, \tag{2.11}$$

which receives contributions from all terms contained in the correlation function. However, it incorporates high-dimensional condensates that are not directly related to the spectral density — a practice that raises doubts about its physical relevance. A more fundamental issue, however, is the ambiguous physical meaning of the PC itself. Within the Borel window, we observe a stark contrast: while the extracted hadron mass remains stable, the PC varies considerably. This presents an internal inconsistency: if the PC were a physically meaningful quantity, it should not be highly sensitive to the unphysical parameter M_B^2, nor should its significant variation leave the mass unaffected.

2.2 The conventional moment QCD sum rules

The MSR follows essentially the same procedure with LSR, differing only slightly on the phenomenological side. Instead of performing the Borel transformation, one defines the following moments by taking derivatives of the correlation function $\Pi(q^2)$ in the Euclidean region $Q^2 \equiv -q^2 > 0$ [3]

$$M_n(Q_0^2) = \frac{1}{\Gamma(n+1)} \left(-\frac{\mathrm{d}}{\mathrm{d}Q^2}\right)^n \Pi(Q^2)|_{Q^2=Q_0^2}. \tag{2.12}$$

On the quark-gluon side, the moment $M_n(Q_0^2)$ can be obtained from the OPE, just as in the LSR

$$\begin{aligned} \Pi^{\mathrm{OPE}}(q^2) &= \int_{s_N}^{\infty} \frac{\rho^{\mathrm{OPE}}(s)}{s-q^2}\mathrm{d}s + \Pi^{\mathrm{NS}}(q^2), \\ M_n^{\mathrm{OPE}}(Q_0^2) &= \int_{s_N}^{\infty} \frac{\rho^{\mathrm{OPE}}(s)}{(s+Q_0^2)^{n+1}}\mathrm{d}s + M_n^{\mathrm{NS}}(Q_0^2), \\ M_n^{\mathrm{NS}}(Q_0^2) &= \frac{1}{\Gamma(n+1)} \left(-\frac{\mathrm{d}}{\mathrm{d}Q^2}\right)^n \Pi^{\mathrm{NS}}(q^2)|_{Q^2=Q_0^2}. \end{aligned} \tag{2.13}$$

Using Eq.(2.4), one can write the moment function on the phenomenological side as

$$\begin{aligned} M_n^{\mathrm{PH}}(Q_0^2) &= \frac{f_X^2}{(m_X^2+Q_0^2)^{n+1}}[1+\delta_n(s_h,Q_0^2)], \\ \delta_n(s_h,Q_0^2) &:= \frac{(m_X^2+Q_0^2)^{n+1}}{f_X^2}\int_{s_h}^{\infty} \frac{\rho^h(s)}{(s+Q_0^2)^{n+1}}\mathrm{d}s, \end{aligned} \tag{2.14}$$

in which $\delta_n(s_h, Q_0^2)$ contains the contributions of higher excited states. To eliminate the coupling f_X in Eq.(2.14), we consider the following ratio of the moments

$$r^{\mathrm{PH}}(n,Q_0^2) = \frac{M_n^{\mathrm{PH}}(Q_0^2)}{M_{n+1}^{\mathrm{PH}}(Q_0^2)} = (m_X^2+Q_0^2)\frac{1+\delta_n(s_h,Q_0^2)}{1+\delta_{n+1}(s_h,Q_0^2)}. \tag{2.15}$$

On the OPE side, the same ratio can be considered

$$r^{\mathrm{OPE}}(n,Q_0^2) = \frac{M_n^{\mathrm{OPE}}(Q_0^2)}{M_{n+1}^{\mathrm{OPE}}(Q_0^2)}. \tag{2.16}$$

Both sides should yield the same result

$$r^{\mathrm{OPE}}(n,Q_0^2) = r^{\mathrm{PH}}(n,Q_0^2). \tag{2.17}$$

The moment approach also relies on an additional approximation. According to conventional wisdom, for sufficiently large n, one expects that $\delta_n(s_h, Q_0^2) \approx \delta_{n+1}(s_h, Q_0^2)$ for convergence. Hence, the rightmost part of Eq. (2.15) simplifies to

$$r^{\mathrm{PH}}(n,Q_0^2) = m_X^2 + Q_0^2. \tag{2.18}$$

Then the hadron mass of the lowest-lying resonance m_X can be immediately extracted as

$$m_X(n,Q_0^2) = \sqrt{r^{\mathrm{OPE}}(n,Q_0^2) - Q_0^2}. \tag{2.19}$$

Both the MSR and LSR can be used to extract the ground state hadron mass. However, Eq. (2.14) reveals a drawback of the MSR approach: the lack of knowledge of both $\rho^h(s)$ and $\delta_n(s_h, Q_0^2)$ prevents the determination of the coupling f_X. A more striking issue is the systematic discrepancy between the two methods: the conventional MSR consistently yields a larger mass prediction than LSR.

Motivated by these observations, we introduce in the next section an improved version of the moment sum rules that simultaneously resolves all of these issues.

3 The improved moment QCD sum rules

In this section, we establish the formalism of the improved moment QCD sum rules. We discuss its key idea and basic procedure, while deferring the illustrative examples to the next section.

3.1 Motivation and core idea

To begin with, it is instructive to examine why the conventional MSR systematically yields a larger hadron mass compared with the LSR's result.

By labeling the correlation function as "OPE" and "PH" in Sec. 2, we have explicitly indicated that the approximation $\delta_n(s_h, Q_0^2) \approx \delta_{n+1}(s_h, Q_0^2)$ is imposed solely on the phenomenological side, leaving the OPE side intact. A comparison of Eq. (2.8) with Eq. (2.13) reveals a crucial difference: in the MSR, the integration over the OPE spectral density $\rho^{\rm OPE}(s)$ extends to infinity, whereas in the LSR, the integral is effectively cut off at the duality parameter s_0. This distinction implies that the ground state hadron mass m_X extracted from the MSR inevitably receives contamination from higher excited states, which naturally shifts the extracted mass upward. The difference in the upper limit of integration ultimately originates from the implementation of quark-hadron duality, which is explicitly enforced in the LSR but not in the moment approach.

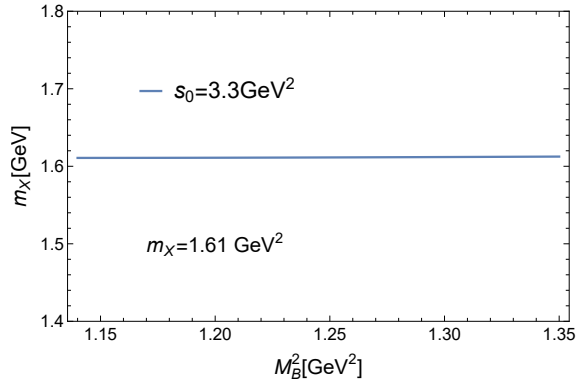

Figure 1. Mass extracted from the OPE Eq. (4.2) in Laplace sum rules. The scale s_0 is taken to be $3.3\,\mathrm{GeV}^2$

An important observation is that the mass discrepancy between the LSR and MSR can be resolved simply by adopting the same duality parameter s_0. To illustrate this, we

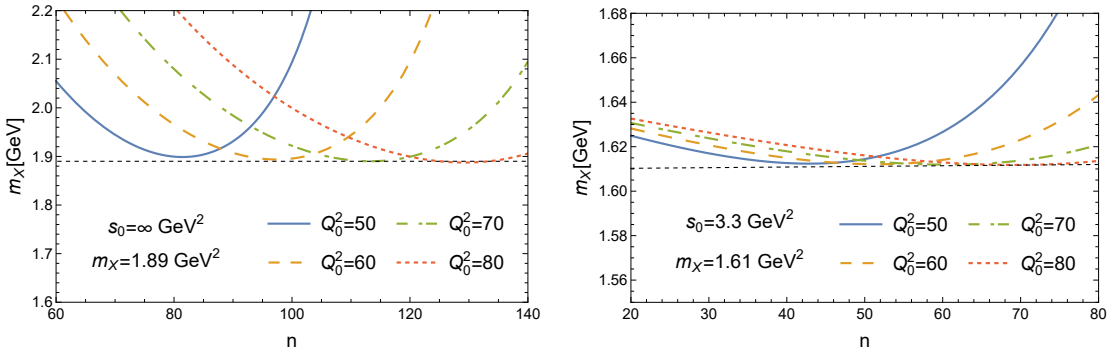

(a) (b)

Figure 2. Mass extracted from the OPE Eq. (4.2) in moment sum rules. The upper limit of integration in Eq. (2.13) is taken as infinity in Fig.2(a) and as 3.3 GeV^2 in Fig.2(b).

compare in Figs. 1 and 2 the numerical results obtained from the two methods for the pseudoscalar tetraquark state $ud\bar{d}\bar{s}$, with its OPE expression given in Eq. (4.2). When each method is analyzed with its own independently optimized parameters, the MSR mass is about 0.3 GeV higher than the LSR mass. However, when both methods are evaluated with the same duality parameter, $s_0 = 3.3$ GeV^2, the extracted masses converge to approximately 1.61 GeV.

Given the above discussion, it is essential that quark-hadron duality be incorporated into the MSR as well, in order to ensure an accurate extraction of the lowest-lying hadron mass. Accordingly, the moment of the correlation function in Eq. (2.13) can be written as

$$\begin{aligned} M_n^{\rm OPE}(Q_0^2) &= \int_{s_N}^{s_0} \frac{\rho^{\rm OPE}(s)}{(s+Q_0^2)^{n+1}}{\rm d}s + \int_{s_0}^{\infty} \frac{\rho^{\rm OPE}(s)}{(s+Q_0^2)^{n+1}}{\rm d}s + M_n^{\rm NS}(Q_0^2), \\ \tilde{M}_n^{\rm OPE}(s_0,Q_0^2) &:= \int_{s_N}^{s_0} \frac{\rho^{\rm OPE}(s)}{(s+Q_0^2)^{n+1}}{\rm d}s + M_n^{\rm NS}(Q_0^2), \\ M_n'^{\rm OPE}(s_0,Q_0^2) &:= \int_{s_0}^{\infty} \frac{\rho^{\rm OPE}(s)}{(s+Q_0^2)^{n+1}}{\rm d}s. \end{aligned} \tag{3.1}$$

After incorporating quark–hadron duality, the moment function decomposes into two contributions $\tilde{M}_n^{\rm OPE}(s_0,Q_0^2)$ and $M_n'^{\rm OPE}(s_0,Q_0^2)$. According to Eq. (2.6), $M_n'^{\rm OPE}(s_0,Q_0^2)$ satisfies:

$$M_n'^{\rm OPE}(s_0,Q_0^2) = \int_{s_0}^{\infty} \frac{\rho^{\rm OPE}(s)}{(s+Q_0^2)^{n+1}}{\rm d}s = \int_{s_h}^{\infty} \frac{\rho^{h}(s)}{(s+Q_0^2)^{n+1}}{\rm d}s. \tag{3.2}$$

Subsequently, we can rewritten Eq. (2.17) as

$$\frac{\tilde{M}_n^{\rm OPE}(s_0,Q_0^2) + M_n'^{\rm OPE}(s_0,Q_0^2)}{\tilde{M}_{n+1}^{\rm OPE}(s_0,Q_0^2) + M_{n+1}'^{\rm OPE}(s_0,Q_0^2)} = (m_X^2+Q_0^2)\frac{1+\delta_n(s_h,Q_0^2)}{1+\delta_{n+1}(s_h,Q_0^2)}. \tag{3.3}$$

To maintain a uniform formalism, we define the function $\delta_n'(s_0,Q_0^2)$ as

$$\delta_n'(s_0,Q_0^2) := \frac{M_n'^{\rm OPE}(s_0,Q_0^2)}{\tilde{M}_n^{\rm OPE}(s_0,Q_0^2)}, \tag{3.4}$$

so that Eq. (3.3) can be expressed as

$$\frac{\tilde{M}_n^{\rm OPE}(s_0,Q_0^2)}{\tilde{M}_{n+1}^{\rm OPE}(s_0,Q_0^2)}\frac{1+\delta'_n(s_0,Q_0^2)}{1+\delta'_{n+1}(s_0,Q_0^2)}=(m_X^2+Q_0^2)\frac{1+\delta_n(s_h,Q_0^2)}{1+\delta_{n+1}(s_h,Q_0^2)}. \tag{3.5}$$

The conventional MSR approach employs a key approximation: $\delta_n(s_h,Q_0^2)\approx\delta_{n+1}(s_h,Q_0^2)$ for sufficiently large n. Under this assumption, the phenomenological representation retains only the ground-state contribution, whereas the OPE side continues to include contributions from higher excited states. Imposing the quark-hadron duality in Eq. (3.2), which gives $\delta'_n(s_0,Q_0^2)=\delta_n(s_h,Q_0^2)$, consistency demands that $\delta'_n(s_0,Q_0^2)\approx\delta'_{n+1}(s_0,Q_0^2)$ to ensure a reliable extraction of the mass of the lowest-lying state. This condition is the foundation of the IMSR approach proposed in this work

Incorporating the two approximations yields the mass formula

$$m_X^2(s_0,Q_0^2,n)=\frac{\tilde{M}_n^{\rm OPE}(s_0,Q_0^2)}{\tilde{M}_{n+1}^{\rm OPE}(s_0,Q_0^2)}-Q_0^2. \tag{3.6}$$

Compared with the conventional MSR in Eq. (2.19), the improved expression in Eq. (3.6) differs only in that the upper limit of integration in the moment function is now truncated at the scale s_0.

Unlike the unknown $\delta_n(s_h,Q_0^2)$, the quantity $\delta'_n(s_0,Q_0^2)$ can be determined analytically (or numerically) from the OPE. Given that $\rho^{\rm OPE}(s)$ is known, $\delta'_n(s_0,Q_0^2)$ depends on the free parameters (s_0,Q_0^2,n). The approximation $\delta'_n(s_0,Q_0^2)\approx\delta'_{n+1}(s_0,Q_0^2)$ thus provides a posteriori constrain on s_0.

It should be further emphasized that $\delta_n(s_h,Q_0^2)\approx\delta_{n+1}(s_h,Q_0^2)$ on the phenomenological side is not merely an approximation. In effect, the transition from eq. (2.15) to eq. (2.18) demands that $\delta_n(s_h,Q_0^2)$ and $\delta_{n+1}(s_h,Q_0^2)$ be strictly equal. Consistency then requires $\delta'_n(s_0,Q_0^2)=\delta'_{n+1}(s_0,Q_0^2)$ on the OPE side as well. In practice, however, the exact equality cannot be achieved exactly, as the parameters (s_0,Q_0^2,n) are inherently finite in any numerical implementation. We will therefore enforce this condition in an approximate sense by means of a fitting procedure, which will be detailed in the following.

In the IMSR framework, we are able to calculate the coupling f_X by using the quark-hadron duality

$$\int_{s_N}^{s_0}\frac{\rho^{\rm OPE}(s)}{s-q^2}+\Pi^{\rm NS}(q^2)=\frac{f_X^2}{m_X^2-q^2}. \tag{3.7}$$

Taking the n-th moment of both sides

$$\tilde{M}_n^{\rm OPE}(s_0,Q_0^2)=\frac{f_X^2}{(m_X^2+Q_0^2)^{n+1}}, \tag{3.8}$$

so that the coupling f_X can then be determined as

$$f_X^2=(m_X^2+Q_0^2)^{n+1}\tilde{M}_n^{\rm OPE}(s_0,Q_0^2). \tag{3.9}$$

It is clear that the coupling f_X depends on the hadron mass m_X, and both of them must be evaluated with the same set of parameters (s_0,Q_0^2,n).

3.2 Dependence conditions

Before presenting the implementation of the IMSR, it is necessary to clarify which of the parameters (s_0, Q_0^2, n) in Eq. (3.6) are physical and unphysical. This distinction will be crucial for correctly defining the dependence conditions and establishing the appropriate stability criteria in the subsequent analysis.

- The upper integration limit s_0 in Eq. (3.6) truncates the high-energy region and is therefore physical, as it determines how much of the physical spectrum is retained on the OPE side. In the conventional MSR, however, convergence of the integral is ensured by the large value of Q_0^2 and n-th derivative of the correlation function $\Pi(q^2)$, which together suppress contributions from higher excited states. This guarantees convergence even in the limit $s_0 \to \infty$, as illustrated in Fig. 2(a).

- The parameter Q_0^2 is the Euclidean momentum at which the correlation function and its derivatives are evaluated. On grounds of analyticity, the OPE and phenomenological representations are expected to agree for any $Q_0^2 > 0$, as long as Q_0^2 is large enough to guarantee the convergence of the OPE series. Consequently, the choice of Q_0^2 is essentially arbitrary and thus it should be an unphysical auxiliary variable.

- Similarly, n must be chosen sufficiently large so that the approximations $\delta_n(s_h, Q_0^2) \approx \delta_{n+1}(s_h, Q_0^2)$ and $\delta_n'(s_0, Q_0^2) \approx \delta_{n+1}'(s_0, Q_0^2)$. Hence, the specific choice of n is therefore arbitrary and carries no physical significance.

With the above discussions, one finds that the extracted mass m_X should exhibit stability with respect to variations in both Q_0^2 and n. In practice, we can formulate the conditions of parametric dependence that the improved mass formula in Eq. (3.6) should satisfy:

$$\begin{aligned}
\left|\frac{\partial m_X^2(s_0, Q_0^2, n)}{\partial Q_0^2}\right| &= \left|\frac{1}{\tilde{M}_{n+1}^2}\left(\tilde{M}_{n+1}\frac{\partial \tilde{M}_n}{\partial Q_0^2} - \tilde{M}_n\frac{\partial \tilde{M}_{n+1}}{\partial Q_0^2} - \tilde{M}_{n+1}^2\right)\right| \leq \epsilon_Q, \\
\left|\frac{\partial m_X^2(s_0, Q_0^2, n)}{\partial n}\right| &= \left|\frac{1}{\tilde{M}_{n+1}^2}\left(\tilde{M}_{n+1}\frac{\partial \tilde{M}_n}{\partial n} - \tilde{M}_n\frac{\partial \tilde{M}_{n+1}}{\partial n}\right)\right| \leq \epsilon_n \text{ GeV}^2,
\end{aligned} \tag{3.10}$$

in which ϵ_Q and ϵ_n are two small tolerance parameters. The practical importance of Eq. (3.10) lies in its ability to provide a quantitative measure of parametric dependences, thereby offering a well-defined criterion for assessing the reliability of the extracted mass against variations in the auxiliary parameters. Assuming that Q_0^2 and n similarly affect the mass m_X, we shall adopt $\epsilon_Q = \epsilon_n = \epsilon$ in the following section for simplicity and without loss of generality

$$\left|\frac{\partial m_X^2(s_0, Q_0^2, n)}{\partial Q_0^2}\right| \leq \epsilon, \qquad \left|\frac{\partial m_X^2(s_0, Q_0^2, n)}{\partial n}\right| \leq \epsilon \text{ GeV}^2, \tag{3.11}$$

where ϵ is dimensionless and its specific value will be discussed later.

3.3 General procedure

In this subsection, we demonstrate how the approximation and dependence conditions enable a unique determination of both s_0 and the mass m_X, without invoking any subjective criteria.

We begin by choosing a trial interval $[n_0, n_1]$ for the integer parameter n. For fixed s_0 and n, the conditions in Eq. (3.11) constrain Q_0^2 to a finite range, thereby obviating the need for an a priori interval for this variable. Although Q_0^2 is continuous in principle, we discretize it with a grid spacing of $\frac{1}{2}$ GeV^2 for numerical analyses throughout this work.

We next select a suitable value of ϵ and investigate, for a range of s_0 values, whether Eq. (3.11) admits solutions for Q_0^2 within the chosen interval $n \in [n_0, n_1]$. When s_0 is significantly removed from its physical value — say $s_0 = 2$ or 8 GeV^2 as opposed to the expected vicinity of 5 GeV^2 — the conditions in Eq. (3.11) are generally not satisfied. This behavior provides a practical means of identifying the approximate range in which s_0 must reside.

Decreasing the value of ϵ imposes progressively stricter dependence conditions, which in turn narrows the viable interval for s_0. This behavior is advantageous: it reduces the computational cost of subsequent analyses and simultaneously removes unphysical regions from the parameter space. To determine a suitable ϵ, we adopt an iterative strategy, beginning with a relatively loose threshold (e.g., $\epsilon = 10^{-3}$) and gradually tightening it (e.g., to $\epsilon = 10^{-4}$), while observing the corresponding contraction of the acceptable s_0 region.

To quantify the approximation, we define the function $\eta(s_0, Q_0^2, n)$ as

$$\eta(s_0, Q_0^2, n) = \frac{\delta'_n(s_0, Q_0^2)}{\delta'_{n+1}(s_0, Q_0^2)}. \tag{3.12}$$

As discussed above, deriving Eq. (3.6) from Eq. (3.5) requires that

$$\eta(s_0, Q_0^2, n) = 1, \tag{3.13}$$

which can be realized only in the limit $n \to \infty$, i.e.

$$\lim_{n\to\infty} \frac{\delta'_n(s_0, Q_0^2)}{\delta'_{n+1}(s_0, Q_0^2)} = 1. \tag{3.14}$$

Noting that $\eta(s_0, Q_0^2, n)$ is strictly monotonically decreasing with respect to n, which implies $\eta > 1$ for all finite values of $n > 0$. The proof of this important property is deferred to Appendix A. This monotonic behavior is precisely the reason why we choose to scan over a trial range of n rather than over Q_0^2 in our numerical procedure.

After determining the parameter space (s_0, Q_0^2, n) that satisfies the dependence condition Eq. (3.11) within a given interval $[n_0, n_1]$, we locate the minimum of $\eta(s_0, Q_0^2, n)$ and denote it by $\eta_{\min}$, with the accompanying value s_0. By scanning over successive intervals $[n_i, n_{i+1}]$ for $i = 1, 2, 3...$, we build up the sequence $(\eta^i_{\min}, s^i_0)$. Because n is restricted to finite integers in each interval, $\eta_{\min}$ remains strictly greater than unity. We then perform a fit

of s_0 against $\eta_{\min}$ and extrapolate the resulting curve to the limiting point $\eta_{\min} = 1$,thereby determining the limiting value of s_0 that corresponds to the exact approximation.

Further details of this procedure will be elaborated in the applications presented in Sec.4.

4 Numerical analysis and applications

In this section, we illustrate the IMSR by applying it to a pseudoscalar light tetraquark $ud\bar{d}\bar{s}$ system. Specifically, we employ the following interpolating current with $J^P = 0^-$ introduced in Ref. [28]

$$P_6 = u_a^T \mathcal{C}\gamma_\mu\gamma_5 d_b[\bar{d}_a\gamma_\mu\mathcal{C}\bar{s}_b^T + (a \leftrightarrow b)], \tag{4.1}$$

where u, d, s are up, down and strange quark fields respectively, and $\mathcal{C} = \mathrm{i}\gamma_2\gamma_0$ is the charge conjugation operator. The correlation function up to dimension-8 reads

$$\begin{aligned}\Pi_{P_6}^{\mathrm{OPE}}(q^2) = \ln\left(\frac{-q^2}{\mu^2}\right)\Bigg[&\frac{-q^8}{7680\pi^6} - \left(\frac{m_s\langle\bar{s}s\rangle}{48\pi^4} - \frac{m_s\langle\bar{q}q\rangle}{48\pi^4} + \frac{5\langle g^2G^2\rangle}{3072\pi^6}\right)q^4 - \left(\frac{7g^2\langle\bar{s}s\rangle^2}{1296\pi^4}\right.\\ &\left. + \frac{7g^2\langle\bar{q}q\rangle^2}{432\pi^4} - \frac{113\langle g^3fG^3\rangle}{13824\pi^6} - \frac{m_s\langle g\bar{q}G\sigma q\rangle}{128\pi^4} + \frac{7m_s\langle g\bar{s}\sigma Gs\rangle}{384\pi^4} - \frac{\langle\bar{q}q\rangle^2}{6\pi^2} + \frac{\langle\bar{q}q\rangle\langle\bar{s}s\rangle}{6\pi^2}\right)q^2\\ &- \left(\frac{5m_s\langle g^2G^2\rangle\langle\bar{s}s\rangle}{768\pi^4} - \frac{7m_s\langle g^2G^2\rangle\langle\bar{q}q\rangle}{1152\pi^4} - \frac{\langle\bar{q}q\rangle\langle g\bar{q}\sigma Gq\rangle}{24\pi^2} + \frac{\langle g\bar{s}\sigma Gs\rangle\langle\bar{q}q\rangle}{48\pi^2} + \frac{\langle g\bar{q}\sigma Gq\rangle\langle\bar{s}s\rangle}{48\pi^2}\right)\Bigg],\end{aligned} \tag{4.2}$$

where m_s denotes the strange quark mass.

For the numerical analysis, we employ the following set of input parameters, including the quark masses, the strong coupling constant, and the QCD condensates [2, 29–34]:

$$\begin{aligned} m_u = m_d = m_q = 0,\ m_s(2\ \mathrm{GeV}) = 93.5 \pm 0.8\ \mathrm{MeV},\\ \langle\bar{q}q\rangle = -(0.24 \pm 0.01)^3\ \mathrm{GeV}^3, \langle\bar{s}s\rangle = (0.8 \pm 0.1)\langle\bar{q}q\rangle,\\ \langle g\bar{q}\sigma Gq\rangle = (0.8 \pm 0.2)\langle\bar{q}q\rangle\ \mathrm{GeV}^2,\ \langle g\bar{s}\sigma Gs\rangle = (0.8 \pm 0.2)\langle g\bar{q}\sigma Gq\rangle,\\ \langle\alpha_s G^2\rangle = (6.35 \pm 0.35) \times 10^{-2}\ \mathrm{GeV}^4,\ \langle g^3fG^3\rangle = 1.2\langle\alpha_s G^2\rangle\ \mathrm{GeV}^2,\\ m_s(\mu) = m_s(2\ \mathrm{GeV})\left[\frac{\alpha_s(\mu)}{\alpha_s(2\ \mathrm{GeV})}\right]^{\frac{12}{33-2n_f}},\\ \alpha_s = \frac{1}{b_0 t}\left[1 - \frac{b_1}{b_0^2}\frac{\ln t}{t} + \frac{b_1^2(\ln^2 t - \ln t - 1) + b_0 b_2}{b_0^4 t^2}\right],\end{aligned} \tag{4.3}$$

where $t = \log\frac{\mu^2}{\Lambda^2}$, $b_0 = \frac{33-2n_f}{12\pi}$, $b_1 = \frac{153-19n_f}{24\pi^2}$, $b_2 = \frac{2857-\frac{5033}{9}n_f+\frac{325}{27}n_f^2}{128\pi^3}$, $\Lambda = 332\,\mathrm{MeV}$ for the number of quark flavors $n_f = 3$. The strange quark mass is taken in the $\overline{\mathrm{MS}}$ scheme at the scale $\mu = 2\,\mathrm{GeV}$. Given that condensate values are evaluated at the renormalization scale $\mu = 1$ GeV, we accordingly adopt the quark masses at the same scale.

As an initial step, we select a trial range for s_0 and test whether the dependence conditions in Eq. (3.11) can be satisfied. Specifically, we consider $s_0 = 3, 4, 5, 6, 7\ \mathrm{GeV}^2$

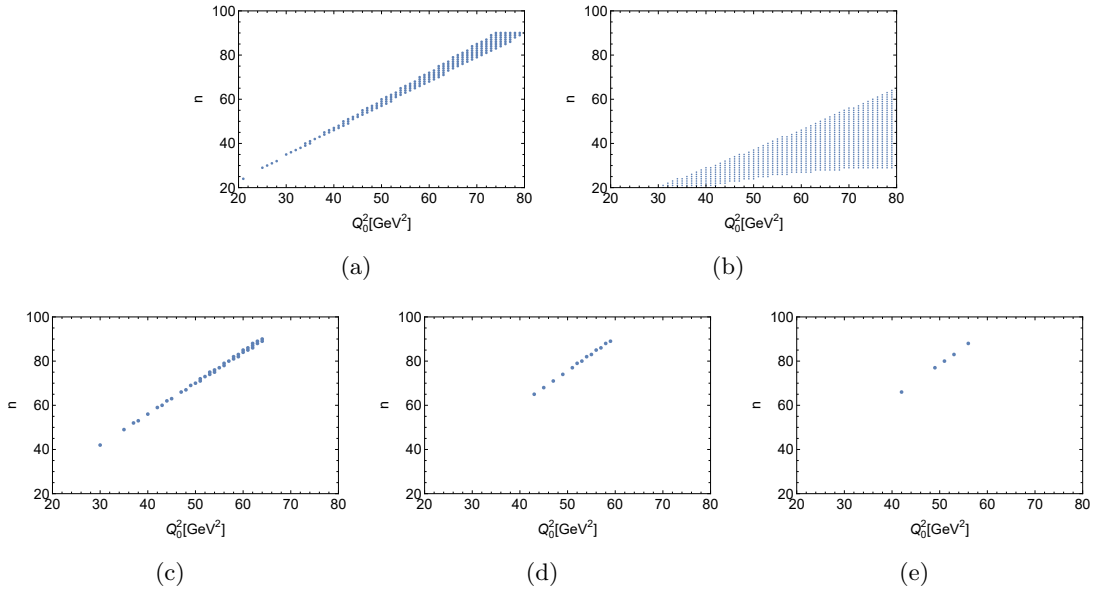

Figure 3. Numerical test of the dependence condition in Eq. (3.11) for the OPE expression in Eq. (4.2), with $\epsilon = 10^{-3}$. Panels (a)–(e) correspond to $s_0 = 3, 4, 5, 6, 7$ GeV^2 , respectively. The marked positions indicate parameter sets that satisfy the dependence condition in Eq. (3.11). The grid spacing for Q_0^2 is 1 GeV^2.

with $\epsilon = 10^{-3}$, and the corresponding results are shown in Fig. 3. It is evident that the admissible parameter space (Q_0^2, n) satisfying Eq. (3.11) attains its maximum extent at $s_0 = 4$ GeV^2. Any deviation of s_0 from this value, whether toward larger or smaller values, reduces the extent of the allowed (Q_0^2, n) region. A more stringent value of ϵ can be adopted to further constrain s_0. With $\epsilon = \frac{1}{4} \times 10^{-3}$, we find that the conditions cannot be fulfilled for any (Q_0^2, n) when $s_0 > 5$ GeV^2.

For $\epsilon = \frac{1}{4} \times 10^{-3}$ and $n \in [60, 80]$, we perform a scan over s_0 with a step size of 0.1 GeV^2, and examine the optimal approximation value $\eta_{\min}$ achievable within the parameter space (s_0, Q_0^2, n). The results are presented in Fig. 4, where a clear minimum is observed at $(s_0^\star, \eta_{\min})$. In other words, the procedure amounts to finding the global minimum of the function $\eta(s_0, Q_0^2, n)$ over the three-dimensional parameter space (s_0, Q_0^2, n), while simultaneously requiring that the dependence conditions in Eq. (3.11) are satisfied.

The initial scan yields a minimum $\eta_{\min} = 1.03921$ at $s_0^\star = 3.5$ GeV^2. Since the scan step size is 0.1 GeV^2, this naturally translates to an uncertainty $s_0^\star = 3.5 \pm 0.1$ GeV^2, avoiding any subjective error estimate. To improve the precision, we then perform a refined scan over the interval $s_0 \in [3.3, 3.7]$ GeV^2 with a reduced step size of 0.02 GeV^2. The refined result, shown in Fig. 5(b), gives $s_0^\star = 3.52 \pm 0.02$ GeV^2 and $\eta_{\min} = 1.03918$.

To assess the sensitivity of $(s_0^\star, \eta_{\min})$ to the choice of the n-intervals, we repeat the same analysis for several alternative ranges: $n \in [40, 60], [80, 100], [100, 120]$, and $[120, 140]$. The resulting curves are displayed in Fig. 5. The slight irregularity observed in the data points is attributable to the discrete nature of the Q_0^2 grid.

The results in Fig. 5 demonstrate that increasing the n-interval systematically reduces

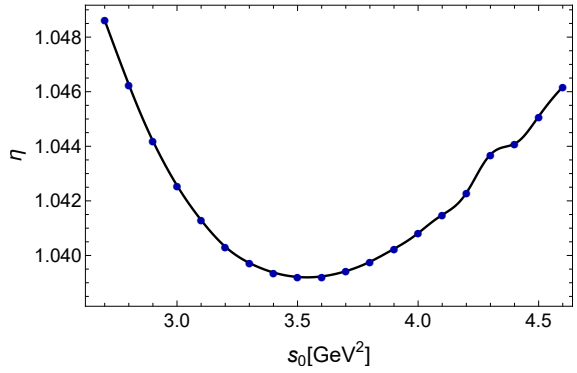

Figure 4. Variation of the approximation function $\eta(s_0, Q_0^2, n)$ with s_0 for $\epsilon = \frac{1}{4} \times 10^{-3}$ and $n \in [60, 80]$.

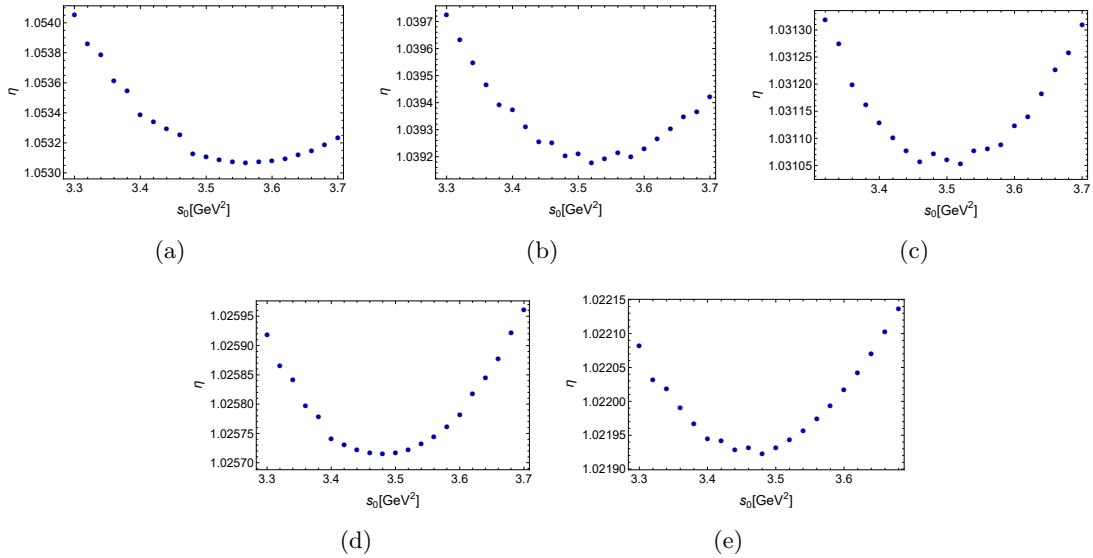

Figure 5. Variations of $\eta(s_0, Q_0^2, n)$ with s_0 for $\epsilon = \frac{1}{4} \times 10^{-3}$ under different n-intervals: (a) $n \in [40, 60]$, (b) $[60, 80]$, (c) $[80, 100]$, (d) $[100, 120]$, (e) $[120, 140]$.

$\eta_{\min}$ while also shifting the location of $s_0^\star$ toward smaller values. By extracting the minimum coordinates $(s_0^\star, \eta_{\min})$ from each curve, we obtain the data points shown in Fig. 6. It is evident from this figure that a larger n-interval corresponds to smaller values of both $\eta_{\min}$ and $s_0^\star$. To determine the value of s_0 at the ideal limit $\eta = 1$, we perform a linear fit $s_0(\eta) = a\eta + b$ to the data points and extrapolate, yielding

$$s_0(\eta = 1) = 3.42 \pm 0.03 \text{ GeV}^2, \tag{4.4}$$

where the uncertainty includes the s_0 step size (0.02 GeV^2) and the linear-fit extrapolation error. The extrapolation is performed over the full n-interval $[40, 140]$, with a step size of $\Delta n = 20$, $\Delta s_0 = 0.02$ GeV^2, and $\epsilon = \frac{1}{4} \times 10^{-3}$.

To verify the robustness of the linear extrapolation, we repeat the entire procedure under two alternative configurations with finer step sizes: (i) $\Delta n = 10$, $\Delta s_0 = 0.01$ GeV^2,

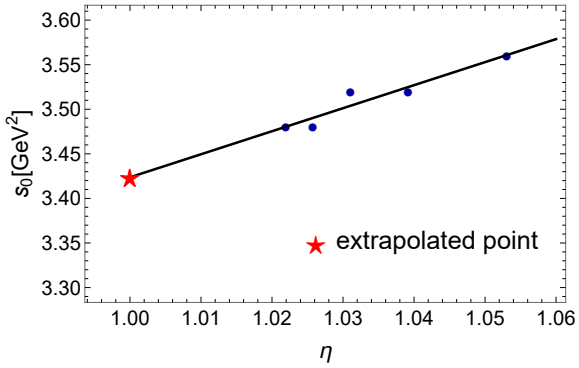

Figure 6. Extracted minima $(s_0^\star, \eta_{\rm min})$ from Fig. 5. The plot illustrates the variation of the minimum position $s_0^\star$ and its corresponding $\eta_{\rm min}$ as the n-interval changes.

$\epsilon = \frac{1}{4} \times 10^{-3}$; and (ii) $\Delta n = 10$, $\Delta s_0 = 0.01$ GeV^2, $\epsilon = 10^{-4}$. The results of these refined analyses are shown in Fig. 7, yielding the extrapolated values $s_0(\eta = 1) = 3.42 \pm 0.02$ GeV^2 and $s_0(\eta = 1) = 3.43 \pm 0.02$ GeV^2, respectively. These values agree well with our previous result, providing strong evidence for the stability and robustness of the extrapolation method. Importantly, the entire determination is essentially free from any ad hoc or subjective assumptions, in contrast to conventional sum rule analyses.

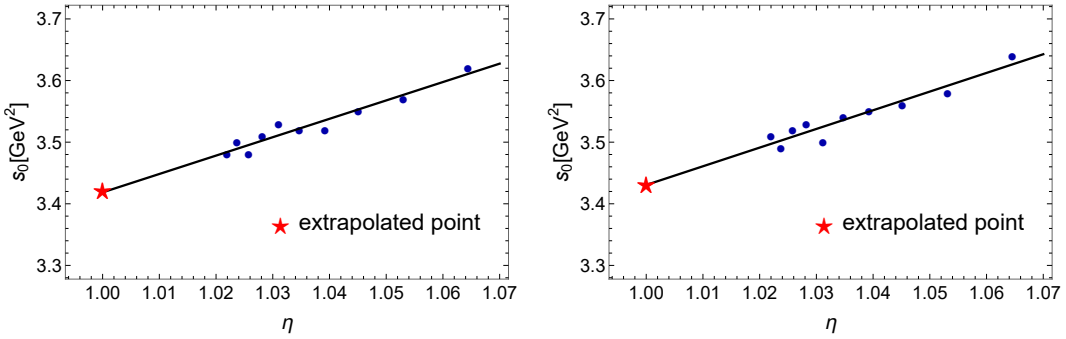

Figure 7. Extrapolation results using $\Delta n = 10$, $\Delta s_0 = 0.01$ GeV^2 for $\epsilon = \frac{1}{4} \times 10^{-3}$ (a) and $\epsilon = 10^{-4}$ (b). The asterisk indicates the extrapolated value at $\eta = 1$.

5 Discussion: Comparison with Laplace sum rules

Both the LSR and the IMSR share a common feature: the suppression of higher excited states. In the LSR, this is accomplished through the Borel transform, which introduces an exponential suppression factor. In the IMSR, the suppression arises from the $n-$th derivative, which provides a polynomial damping. As demonstrated in Figs. 1 and 2, the two methods yield numerically consistent results for the ground-state mass.

Although both the LSR and the IMSR are founded on the principle of quark–hadron duality, a notable distinction arises in how they treat the spectral density in the high-energy

region. In the LSR, the phenomenological spectral density $\rho^h(s)$ above the threshold s_h is explicitly canceled by the OPE spectral density $\rho^{\rm OPE}(s)$ above s_0, effectively isolating the ground-state contribution. However, this cancellation does not come with a built-in criterion for fixing the parameters; one must introduce subjective conditions to constrain the Borel window and duality parameter [1]. Applying the same duality relation directly in the IMSR would lead to the same issue. To overcome this, we adopt the approximation $\delta_n(s_h, Q_0^2) \approx \delta_{n+1}(s_h, Q_0^2)$ from the conventional moment approach. Consistency with the quark-hadron duality then implies that an analogous relation $\delta'_n(s_0, Q_0^2) \approx \delta'_{n+1}(s_0, Q_0^2)$ must also hold on the OPE side.

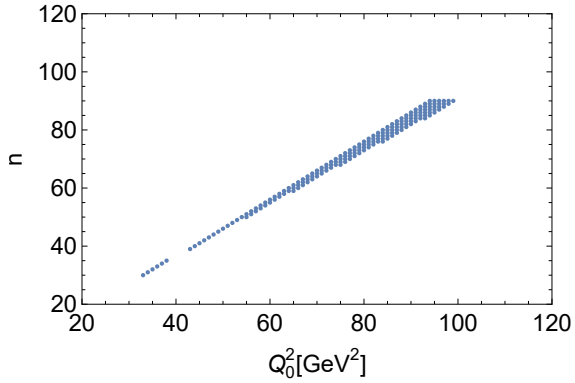

Figure 8. Dependence check for OPE Eq. (4.2) with $\epsilon = \frac{1}{4} \times 10^{-3}$ and $s_0 = 3.42$ GeV^2.

It is also instructive to compare our extracted duality parameter with that obtained via the LSR in our previous work [28]. The present result, $s_0 = 3.42 \pm 0.03$ GeV^2, is fully consistent with the earlier value $s_0 = 3.3 \pm 0.2$ GeV^2. Importantly, however, the earlier determination was subject to the conventional criteria of OPE convergence and pole dominance conditions that are inherently subjective and introduce significant uncertainties. In contrast, the present result is obtained without invoking such ad hoc criteria, rendering it more robust and objective.

It should be emphasized, however, that despite the subjective nature of the conventional criteria, the two methods can still yield essentially consistent results when certain conditions are met. Specifically, if the manually chosen convergence and pole dominance criteria are appropriate, and the extracted mass exhibits minimal dependence on the unphysical Borel parameter, then the LSR and MSR results are in good agreement. To facilitate this assessment, a $\chi^2(s_0)$ function is usually defined to quantify the stability of the hadron mass [36–39]

$$\chi^2(s_0) = \sum_{i=1}^{N} \left[\frac{m_X(s_0, M_{B,i}^2)}{\overline{m}_X(s_0)} - 1 \right]^2, \qquad \overline{m}_X(s_0) = \sum_{i=1}^{N} \frac{m_X(s_0, M_{B,i}^2)}{N}, \tag{5.1}$$

which can provide a more objective basis for selecting the duality parameter.

[1] The Hölder inequality, derived from the positivity of the spectral density [35], provides a formal constraint, but it is relatively weak and can only roughly delimit the allowed parameter region.

A further perspective on the equivalence between the two methods can be gained by examining the parameter space (Q_0^2, n) that satisfies the dependence condition in Eq. (3.11). Specifically, we fix $s_0 = 3.42$ GeV^2 and $\epsilon = \frac{1}{4} \times 10^{-3}$, and identify the parameter space for which the OPE expression in Eq. (4.2) satisfies the dependence condition. The resulting allowed region is shown in Fig. 8, within which the ratio Q_0^2/n remains nearly constant at approximately 1.1 GeV^2. This observation provides a direct connection between the IMSR and LSR frameworks: the constant ratio corresponds to the Borel window 1.14 GeV^2 $\leq M_B^2 \leq$ 1.35 GeV^2 determined in our previous LSR analysis [28].

6 Summary

In this work, we have developed an improved formulation of the moment sum rules. We begin by reexamining the derivations of both the LSR and conventional MSR, and identify their respective limitations: the conventional MSR cannot determine the coupling of the interpolating current, whereas the LSR depends on the ad hoc criteria of OPE convergence and pole dominance, which introduce subjectivity and non-uniqueness. More importantly, the two methods yield inconsistent mass predictions for the ground-state resonance, with the MSR systematically giving larger values.

We demonstrate that this inconsistency originates from the absence of quark-hadron duality in the conventional MSR, which permits contamination from higher excited states on the OPE side and consequently overestimates the ground-state mass. By properly incorporating duality, we derive a new mass formula in Eq. (3.6) within the moment approach.

In this formulation, the approximation $\delta_n(s_h, Q_0^2) \approx \delta_{n+1}(s_h, Q_0^2)$ ensures that only the ground-state resonance is retained on the phenomenological side. On the OPE side, we introduce the corresponding quantity $\delta'_n(s_0, Q_0^2)$. Consistency with quark–hadron duality then naturally requires $\delta'_n(s_0, Q_0^2) \approx \delta'_{n+1}(s_0, Q_0^2)$, which serves as an a posteriori constraint on the parameters. We then classify the three parameters (s_0, Q_0^2, n) in Eq. (3.6) according to whether they are physical or auxiliary. To control the sensitivity to unphysical parameters, we introduce a tolerance parameter ϵ in Eq. (3.11). The combination of the approximation and the dependence conditions leads to a well-defined numerical procedure that uniquely determines both the duality parameter and the ground-state mass, without invoking any ad hoc criteria. The extracted (s_0, m_X) are thus essentially unique.

We illustrate the method by applying it to a pseudoscalar tetraquark $ud\bar{d}\bar{s}$ system. The results are consistent with those obtained from our previous LSR analysis, providing evidence for the equivalence of these two approaches. The IMSR method presented here effectively eliminates the problem of subjectivity that has long plagued the LSR, thereby significantly enhancing the robustness and reliability of QCD sum rule predictions.

Acknowledgments

J.-P. Z. thanks Zi-Xi Ou-Yang, Li-jing Zhang, and Wen-yun Wu for valuable discussions. This work is supported by the National Natural Science Foundation of China under Grant No. 12575153.

A Proof and interpretation of $\eta(s_0, Q_0^2, n) > 1$

In this appendix, we provide a rigorous proof to demonstrate that the approximate function $\eta(s_0, Q_0^2, n) > 1$. Substituting the definition of $\eta(s_0, Q_0^2, n)$ into Eq. (3.6), one obtains the result

$$\eta(s_0, Q_0^2, n) = \frac{1}{m_X^2 + Q_0^2} \frac{\int_{s_0}^{\infty} \frac{\rho^{\mathrm{OPE}}(s)}{(s+Q_0^2)^{n+1}}}{\int_{s_0}^{\infty} \frac{\rho^{\mathrm{OPE}}(s)}{(s+Q_0^2)^{n+2}}}. \tag{A.1}$$

In the limit of $n \to \infty$, the function η approaches unity for a physical spectral function $\rho^{\mathrm{OPE}}(s)$. If we can establish that η is monotonically decreasing with respect to n, it follows directly that $\eta > 1$ for any finite $n > 0$. We investigate the derivative $\mathrm{d}\eta/\mathrm{d}n$ to determine its monotonicity (omitting a positive factor)

$$\begin{aligned} \frac{\mathrm{d}\eta}{\mathrm{d}n} \propto & \int_{s_0}^{\infty} \frac{\rho^{\mathrm{OPE}}(s)\mathrm{d}s}{(s+Q_0^2)^{n+1}} \int_{s_0}^{\infty} \frac{\rho^{\mathrm{OPE}}(s)\ln(s+Q_0^2)\mathrm{d}s}{(s+Q_0^2)^{n+2}} \\ & - \int_{s_0}^{\infty} \frac{\rho^{\mathrm{OPE}}(s)\mathrm{d}s}{(s+Q_0^2)^{n+2}} \int_{s_0}^{\infty} \frac{\rho^{\mathrm{OPE}}(s)\ln(s+Q_0^2)\mathrm{d}s}{(s+Q_0^2)^{n+1}}. \end{aligned} \tag{A.2}$$

We introduce the variable substitution $x = s + Q_0^2$, which changes the integration lower limit to $x_0 = s_0 + Q_0^2$. In terms of this new variable, Eq. (A.2) can be expressed compactly by defining the positive weight function $W(x)$ as

$$W(x) = \frac{\rho^{\mathrm{OPE}}(x - Q_0^2)}{x^{n+2}}. \tag{A.3}$$

Then one can express Eq. (A.2) as

$$\frac{\mathrm{d}\eta}{\mathrm{d}n} \propto \int_{x_0}^{\infty} W(x)\, x\, \mathrm{d}x \int_{x_0}^{\infty} W(x)\, \ln x\, \mathrm{d}x - \int_{x_0}^{\infty} W(x)\, \mathrm{d}x \int_{x_0}^{\infty} W(x)\, x \ln x\, \mathrm{d}x. \tag{A.4}$$

We then apply the Chebyshev's integral inequality to determine the positive definiteness of $\mathrm{d}\eta/\mathrm{d}n$. For two functions $f(x)$ and $g(x)$ of identical monotonicity on the interval $[a, b]$, and a Weight function $W(x) \geq 0$, the Chebyshev's integral inequality takes the form

$$\int_a^b W(x)\mathrm{d}x \int_a^b W(x) f(x) g(x)\mathrm{d}x \geq \int_a^b W(x) f(x)\mathrm{d}x \int_a^b W(x) g(x)\mathrm{d}x, \tag{A.5}$$

in which the equality holds only if at least one of the functions $f(x)$ and $g(x)$ is constant.

Before applying Chebyshev's inequality, we verify its prerequisites: $Q_0^2 > 0$, $n > 0$, and n chosen larger than the highest power in $\rho^{\mathrm{OPE}}(s)$ to ensure convergence. The weight function $W(x)$ is positive for $s > s_0$ since $\rho^{\mathrm{OPE}}(s) > 0$. This is physically guaranteed; otherwise, the ground-state mass would be determined by an unphysical negative-definite spectral density.

To apply the Chebyshev's integral inequality in Eq. (A.5), we define $f(x) = x$ and $g(x) = \ln(x)$, both of which are strictly increasing on the interval $[x_0, \infty]$, and hence they share the same monotonicity. The conditions required by the inequality are therefore fully satisfied, and we obtain

$$\int_{x_0}^{\infty} W(x)\mathrm{d}x \int_{x_0}^{\infty} W(x) x \ln x \mathrm{d}x > \int_{x_0}^{\infty} W(x) x \mathrm{d}x \int_{x_0}^{\infty} W(x) \ln x \mathrm{d}x. \tag{A.6}$$

According Eq. (A.2), this result leads to

$$\frac{\mathrm{d}\eta}{\mathrm{d}n} < 0. \tag{A.7}$$

This establishes that $\eta(s_0, Q_0^2, n)$ is strictly monotonically decreasing with respect to n, while $\eta > 1$ for any finite $n > 0$.

References

[1] M.A. Shifman, A.I. Vainshtein and V.I. Zakharov, *QCD and Resonance Physics. Theoretical Foundations*, *Nucl. Phys. B* **147** (1979) 385.

[2] M.A. Shifman, A.I. Vainshtein and V.I. Zakharov, *QCD and Resonance Physics: Applications*, *Nucl. Phys. B* **147** (1979) 448.

[3] L.J. Reinders, H. Rubinstein and S. Yazaki, *Hadron Properties from QCD Sum Rules*, *Phys. Rept.* **127** (1985) 1.

[4] H.-X. Chen, W. Chen, X. Liu and S.-L. Zhu, *The hidden-charm pentaquark and tetraquark states*, *Phys. Rept.* **639** (2016) 1 [1601.02092].

[5] R.F. Lebed, R.E. Mitchell and E.S. Swanson, *Heavy-Quark QCD Exotica*, *Prog. Part. Nucl. Phys.* **93** (2017) 143 [1610.04528].

[6] A. Esposito, A. Pilloni and A.D. Polosa, *Multiquark Resonances*, *Phys. Rept.* **668** (2017) 1 [1611.07920].

[7] F.-K. Guo, C. Hanhart, U.-G. Meißner, Q. Wang, Q. Zhao and B.-S. Zou, *Hadronic molecules*, *Rev. Mod. Phys.* **90** (2018) 015004 [1705.00141].

[8] Y.-R. Liu, H.-X. Chen, W. Chen, X. Liu and S.-L. Zhu, *Pentaquark and Tetraquark states*, *Prog. Part. Nucl. Phys.* **107** (2019) 237 [1903.11976].

[9] N. Brambilla, S. Eidelman, C. Hanhart, A. Nefediev, C.-P. Shen, C.E. Thomas et al., *The XYZ states: experimental and theoretical status and perspectives*, *Phys. Rept.* **873** (2020) 1 [1907.07583].

[10] H.-X. Chen, W. Chen, X. Liu, Y.-R. Liu and S.-L. Zhu, *An updated review of the new hadron states*, *Rept. Prog. Phys.* **86** (2023) 026201 [2204.02649].

[11] L. Meng, B. Wang, G.-J. Wang and S.-L. Zhu, *Chiral perturbation theory for heavy hadrons and chiral effective field theory for heavy hadronic molecules*, *Phys. Rept.* **1019** (2023) 1 [2204.08716].

[12] M.-Z. Liu, Y.-W. Pan, Z.-W. Liu, T.-W. Wu, J.-X. Lu and L.-S. Geng, *Three ways to decipher the nature of exotic hadrons: Multiplets, three-body hadronic molecules, and correlation functions*, *Phys. Rept.* **1108** (2025) 1 [2404.06399].

[13] Z.-G. Wang, *Review of the QCD sum rules for exotic states*, *Front. Phys. (Beijing)* **21** (2026) 016300 [2502.11351].

[14] D.B. Leinweber, *QCD sum rules for skeptics*, *Annals Phys.* **254** (1997) 328 [nucl-th/9510051].

[15] A. Carvunis, F. Mahmoudi and Y. Monceaux, *Potential of light-cone sum rules without semiglobal quark-hadron duality*, *Phys. Rev. D* **110** (2024) 114008 [2404.01290].

[16] H.-n. Li and H. Umeeda, *QCD sum rules with spectral densities solved in inverse problems*, *Phys. Rev. D* **102** (2020) 114014 [2006.16593].

[17] A.-S. Xiong, T. Wei and F.-S. Yu, *Inverse Problem Approach for Non-Perturbative QCD: Foundation*, 2211.13753.

[18] H.-n. Li, *Dispersive analysis of glueball masses*, *Phys. Rev. D* **104** (2021) 114017 [2109.04956].

[19] H.-n. Li, *Dispersive derivation of the pion distribution amplitude*, *Phys. Rev. D* **106** (2022) 034015 [2205.06746].

[20] H.-n. Li, *Dispersive Analysis of Excited Glueball States*, *Chin. Phys. Lett.* **41** (2024) 101101 [2408.06738].

[21] Z.-X. Zhao, Y.-P. Xing and R.-H. Li, *A progress in the inverse matrix method in QCD sum rules*, *Eur. Phys. J. C* **84** (2024) 1105 [2407.09819].

[22] Z.-X. Ou-Yang, P. Gubler, M. Oka, G.-J. Wang and J.-J. Wu, *Resonance sum rules: An application to the square-well potential*, *Phys. Rev. D* **112** (2025) 114034 [2509.24336].

[23] P. Colangelo and A. Khodjamirian, *QCD sum rules, a modern perspective*, hep-ph/0010175.

[24] T. Kojo, A. Hayashigaki and D. Jido, *Pentaquark state in pole-dominated QCD sum rules*, *Phys. Rev. C* **74** (2006) 045206 [hep-ph/0602004].

[25] W. Lucha, D. Melikhov and S. Simula, *Systematic uncertainties of hadron parameters obtained with QCD sum rules*, *Phys. Rev. D* **76** (2007) 036002 [0705.0470].

[26] M.A. Shifman, *Quark hadron duality*, in *8th International Symposium on Heavy Flavor Physics*, vol. 3, (Singapore), pp. 1447–1494, World Scientific, 7, 2000, DOI [hep-ph/0009131].

[27] M. Shifman, *QCD sum rules: Bridging the gap between short and large distances*, *Nucl. Phys. B Proc. Suppl.* **207-208** (2010) 298 [1101.1122].

[28] J.-P. Zhang, X.-L. Chen, Z.-X. Ou-Yang, X. Yu, W. Chen and J.-J. Wu, *Unraveling K(1690) as a pseudoscalar $udd\bar{s}\bar{}$ tetraquark state*, *Phys. Rev. D* **112** (2025) 094047 [2507.05726].

[29] Particle Data Group collaboration, *Review of particle physics*, *Phys. Rev. D* **110** (2024) 030001.

[30] S. Narison, *QCD parameter correlations from heavy quarkonia*, *Int. J. Mod. Phys. A* **33** (2018) 1850045 [1801.00592].

[31] S. Narison, *QCD condensates and αs from τ-decay: Summary*, *J. Subatomic Part. Cosmol.* **3** (2025) 100038 [2501.08369].

[32] H.Y. Jin, J.G. Korner and T.G. Steele, *Improved determination of the mass of the 1-+ light hybrid meson from QCD sum rules*, *Phys. Rev. D* **67** (2003) 014025 [hep-ph/0211304].

[33] Z.-R. Huang, H.-Y. Jin and Z.-F. Zhang, *New predictions on the mass of the 1^{-+} light hybrid meson from QCD sum rules*, *JHEP* **04** (2015) 004 [1411.2224].

[34] A. Di Giacomo, K. Fabricius and G. Paffuti, *Trilinear Gluon Condensation Parameter From Lattice QCD*, *Phys. Lett. B* **118** (1982) 129.

[35] M. Benmerrouche, G. Orlandini and T.G. Steele, *Constraints on QCD sum rules from the Holder inequalities*, *Phys. Lett. B* **356** (1995) 573 [hep-ph/9507304].

[36] G.-F. Xu, X.-L. Chen, J.-P. Zhang, N. Li and W. Chen, *Possible bound states in the triple-η_c and triple-J/ψ systems*, *Chin. Phys. Lett.* **42** (2025) 070201 [2504.08665].

[37] S.-H. Li, W.-Y. Lai and H.-Y. Jin, *Probing Excited $q\bar{q}$ Mesons via QCD Sum Rules*, 2512.16637.

[38] S.-H. Li, Z.-R. Huang, W. Chen and H.-Y. Jin, *Revising the mass of light hybrid mesons: NLO QCD sum rules point to $\phi(2170)$ as a prime candidate*, *JHEP* **03** (2026) 087 [2506.22412].

[39] Z.-Z. Chen, X.-L. Chen, P.-F. Yang and W. Chen, *P-wave fully charm and fully bottom tetraquark states*, *Phys. Rev. D* **109** (2024) 094011 [2402.03117].